NASA Technical Memorandum

November 2002

Modeling Rotor Harmonics

R. E. McFarland

NASA, AMES Research Center

Moffett Field, CA 04035-1000 USA

National Aeronautics and

Space Administration

CONTENTS

SYMBOLS

A_{0F}, A_{1F}, B_{1F}	*collective, lateral and longitudinal cyclic*
e, e'	*hinge offset and spar length*
m	*segment number*
n	*blade number*
N	*number of blades*
r_m	*m^{th} element's radius from the hub*
S, C	*summed Poisson sine and cosine series*
s_n, c_n	*Poisson sine and cosine seriess*
v	*tangential velocity*
β_n	*flapping angle of blade n*
β_w	*angle of sideslip*
μ	*advance ratio*
λ_n	*advance angle*
η_i	*random variables at all aerodynamic centers (22 per axis)*
ρ	*Poisson parameter*
ψ_n *(rad)*	*azimuth angle of the n^{th} blade*
Ω *(rad/sec)*	*main rotor angular velocity*

MODELING ROTOR HARMONICS

Richard McFarland
Comment: Poisson:poisson.wrd

R. E. McFarland

Ames Research Center

SUMMARY

For rotorcraft research in all flight regimes, nonlinear simulation models have been developed such as Sikorsky's Black Hawk model. Such engineering-level models are expensive to create, validate and maintain. They are also expensive to operate because the high frequencies produced at the blade-element level of modeling require extensive computational resources and small integration intervals. Although rotor harmonics representative of those generated by a rotorcraft are produced by these models, aliased harmonics are also produced. In contrast, the more common disc-plane rotor models are not contaminated by these harmonics. However, they don't even produce the energetic *N*-per-revolution frequency that is fundamental to a rotor system with *N* blades. Hence, independent mathematical relationships are needed for the superimposition of this frequency on a disc-plane rotor model, or for the production of realistic motion cues.

Harmonic frequencies are produced by helicopter rotor systems, and with increased advance ratio comes increased excitation. They are significant because they influence controllability, survivability and maintainability as well as pilot fatigue. Both symbolic representations and numerical simulations of these frequencies imply extensive, nonlinear mathematical models. Because simplified rotor models capable of replicating harmonics have not been available, rotorcraft research using these models has lacked the energetic N/rev frequency. If the resolved components of this harmonic were available, they could produce motion cues for implementation using a seat shaker.

Mathematical relationships are derived to bridge the *N*/rev deficiency by approximating blade dynamics at significant advance ratio. They may be used to augment tip-path plane rotor models and produce frequency content generally associated with more sophisticated models. From an examination of the nonlinear dynamics of rotor blades in a transverse velocity field, the relationships reveal why a tip path plane (or accumulated behavior of the blades "as a system") behaves more like an airfoil than might be expected. The derivations in this research indicate that tip path plane models are valid over a wider range of flight conditions than previously assumed.

DISCUSSION

For some research topics involving the simulation of rotorcraft, relatively simple mathematical models of rotor systems are needed that are nonetheless capable of representing rotary-system dynamics over a wide range of advance ratios. This is not accomplished with conventional rotor disc models known as "tip-path plane" (TPP) models, because the nonlinear relationships producing harmonics are not considered. Fourier series representations are truncated much too early[1] to produce rotor harmonics. Consider the following quotes:

> *"The frequency of these harmonic terms* [4/rev] *is sufficiently high to be of no interest to handling quality investigations."* And: *"Because of these assumptions and simplifications, the results of the analysis are valid only for a limited range of flight conditions."*[2]

The first quote is brought into question, and the second quote represents a frustrating state of affairs that is addressed in this discussion. Understandably, when assumptions are made early in the development of a model, these assumptions tend to haunt the complete developmental cycle. At the blade level of modeling, TPP model development has historically made an initial assumption that the Fourier series may be truncated to just one term. The derivations of this paper,

---

[1] A Simplified Rotor System Mathematical Model for Piloted Flight Dynamics Simulation, Robert T. N. Chen, NASA TM 78575, May 1979.

[2] A Mathematical Model of a Single Main Rotor Helicopter for Piloted Simulation, Peter D. Talbot, Bruce E. Tinling, William A. Decker, and Robert T. N. Chen, NASA TM84281, Sept. 1982, p. 4.

however, show that this assumption is of little consequence to the fidelity of TPP model dynamics. An infinite series of terms is retained here, well representing at least the first *N* Fourier terms at the blade level of modeling. Only in the very last stages of the development, after the mathematical relationships prove the thesis, are approximations made. This sequence contributes to the validation of all previously developed TPP models, expands their apparent range of validity, and provides a simple technique to further embellish them with the important *N*/rev harmonic.

Previously, for full-mission research "rotating blade-element" (RBE) models have been required, although these are rarely available because they are both economically and computationally expensive. TPP models do not generate the high frequencies that are created by the nonlinear physics described in RBE models, although the magnitudes and directions of these frequencies are significant for a number of reasons. The harmonics vary as functions of system variables and controls, and therefore constitute important motion cues to a pilot. Most importantly, these harmonics are separable from the gross orientation of the rotor plane as an aerodynamic disc.

The lowest harmonic delivered by the Black Hawk rotor system is *N*/rev at 17.2 Hz, which is too high for driving most motion simulators. Indeed, *N*/rev is a destructive frequency to the actual flight hardware as well as to motion simulators. Hence, the ideal solution for simulation is to compute and isolate the *N*/rev vector, and then rather than superimpose it on vehicle dynamics to eventually drive a motion system, redirect the separated components to a seat shaker and leave the unaffected vehicle dynamics to drive the motion system. In this respect TPP models have an advantage over RBE models, which are contaminated with intentional harmonics as well as all manner of aliased harmonics. And these harmonics cannot be separated from a RBE model except in specific cases.[3]

Mathematically, rotor harmonics are nonlinear functions of collective and cyclic angles, as well as vehicle airspeed. If blade-level mathematical models and data are not available in simulation, but fundamental rotor harmonics are desired for research purposes or simply for more realism, then they may be approximated using a generating function[4] developed by Poisson, as well as a knowledge of the collective and cyclic angles. Using "Poisson's kernel[5]," blade-level dynamics may be deduced from the orientation of the rotor system in an asymmetric velocity field. Accurate vector harmonics may then be produced at the significant advance ratios of high-speed flight.

In this research a model of individual blade motion is deduced by the orientation of the tip path plane in an asymmetric flow field. Significant blade harmonics are generated and distributed by vector summations over the system of blades. As a basis, this derivation uses a Fourier series representation of the inverse of the tangential velocity of a given element on a blade with a periodic velocity contribution due to the flow field. The pertinent periodic variable is defined as the "advance angle" rather than the more conventional "azimuth angle," and the coefficients at any given advance angle are power series of a function of the "advance ratio." The advance ratio is eventually redefined for the entire rotor disc. It is shown to be much smaller when the assumed functionality accounts for the periodic forcing function on a system of blades.

Mathematical relationships are developed using Poisson's kernel, which is a classical generating function. This kernel is used for describing functions of the tangential velocity. In particular, the inverse of the tangential velocity is a well-known quantity in expressions for an important aerodynamic variable - the angle of attack. However, rather than the angle of attack, in this derivation the flapping angle of a blade is assumed to be the primary variable, despite the fact that only aerodynamic relationships and data could possibly produce one from the other. This substitution is possible because the harmonic power delivered to a rotorcraft is more closely related to blade flapping dynamics than to angles of attack, which without appropriate aerodynamic functions cannot describe blade motion.

There are underlying assumptions in this research. For example, it is assumed that the orientation of the disc plane is sufficient to determine the low frequency forces and moments due to a rotor system. This typical assumption includes all swashplate activity as responses to pilot excitation of transfer functions that model control system logic and other tip path plane dynamics. It should then be understood that for a rotor as a system, harmonics below *N*/rev are not produced. This is easily demonstrated with a nonlinear blade element model. Of course, if the blades were not modeled as being physically identical, then this assumption would not hold. Actual flight hardware never achieves the mathematical purity

---

[3] Quiet Mode for Nonlinear Rotor Models, R. E. McFarland, NASATM 102236, April 1990.

[4] A. de Moivre introduced generating functions in order to solve the general linear recurrence problem, 1730.

[5] Fourier Series, Georgi P. Tolstov, Prentice-Hall, 1962, p. 164.

of this assumption, so pilots are certainly aware of lower harmonics. But they are not considered here, nor have they ever been the subject of research involving real time simulation at Ames Research Center. So, the ramification of a system of blades with identical physical properties is that the equations that develop forces and moments do not suffer from the lack of higher harmonics. Being distinct, higher harmonics do not contribute to gross vehicle motion, and they are separable. This means that they may be independently considered, and superimposed, if desired. The tremendous body of research that has been done with disc models may certainly be "*valid only for a limited range of flight condition[s]*", but that range is much larger than previously assumed.

1.0 The Task

A parameter "ρ" is necessary to define a generating function[6] capable of modeling a flapping angle. This is here called the "Poisson parameter," and although it is mathematically related to a function of the advance ratio (used in the derivations), it is later shown to have applicability over the entire rotor disc as a function of vehicle airspeed. Its magnitude is computed to conform to energy levels from a blade-element model (and the flight hardware). Verification is performed by spectral comparisons with Sikorsky's Black Hawk UH-60 GENHEL model[7] at distinct frequencies, and significant simplifications are uncovered for implementation in real-time TPP simulations.

The energetic harmonics of RBE models have been known to obscure a vehicle's dynamic behavior. Indeed, for the UH-60 model "quiet mode" was developed to clarify certain engineering variables. However, TPP models are assumed herein, and they do not inherently contain rotor harmonics. For optional inclusion or superimposition into TPP models, rotor harmonics are here derived from elementary considerations. They are developed using series techniques that assure rapid coefficient decay beyond *N*/rev. Thus, the higher harmonics vanish rather than alias into a pilot's operational bandwidth. At the blade level of computation all harmonics up to *N*/rev are faithfully reproduced.

Simplified rotor model relationships are developed that bridge the gap between TPPs and RBEs without requiring additional data beyond those of typical TPPs. These relationships, tentatively called PROMO (an acronym for "Poisson Rotor Model"), are intended to augment tip-path plane models, especially for driving seat shakers.

By evaluating functions of Poisson's kernel at a radial evaluation point, the nonlinear properties of blade motion may be approximated by the assumption that angle of attack and flapping are closely related. The gross characteristics of flapping define the tip path plane geometry. In the Black Hawk model the angle of attack may vary wildly along a blade whereas the flapping angle is computed for the entire blade. Of course, extreme variations in angle of attack have correspondingly less influence on flapping angles because of decreased dynamic pressure. Nonetheless, it should be anticipated that once the derivation using flapping angles is completed, Poisson's parameter must be redefined. After the initial derivations and displays, it is revealed that in order to match energy levels with RBE models, the advance ratio is a very small quantity when "the rotor system as a disc" is considered. This fact justifies various approximations.

The integrals of Poisson functions, that may be used to represent flapping over a blade's radial span, are shown to closely approximate summed values obtained using the equal-annuli summation technique. Then it is shown that normalization of this integral produces values that closely approximate evaluations of the integrand at a single radius. The integrand itself may thus be used to represent a normalized integral over a blade. Because of this fact, closed-form summations exist over the entire system of rotor blades, and these summations may also be resolved to any axis. Most importantly, the summation processes yield the harmonic frequencies of a rotor system, which may be mathematically purged of any undesirable harmonic multiples by series truncation.

Along with the tip path plane orientation, a single Poisson parameter is required for the representation of all of the series coefficients, and this parameter is developed as a function of an element's advance ratio. The derivation is actually appropriate for angles of attack at specific blade radii rather than flapping of the blade as a whole. But the nonlinear relationships between angle of attack and flapping are assumed unavailable. Hence, determining the Poisson parameter requires other considerations. Indeed, it is computed to deliver the proper power spectral density at the *N*-per-rev (*N*/rev)

---

[6] Fundamental Algorithms, Vol. 1, Donald E. Knuth, Addison-Wesley Publishing Co., 1973, p. 86.

[7] UH-60A Black Hawk Engineering Simulation Program: Vol. I - Mathematical Model, Howlett, J. J., NASA CR-166309, Dec. 1981.

rotor frequency. Trivially, the proper power spectral density at one-per-rev (1/rev) is assured from the derivation's assumptions.

At the blade level of modeling, PROMO incorporates principles of rotational motion of a blade in a transverse velocity field. At any radial distance the periodic frequencies of nonlinear RBE models are approximated. The dynamics are expressible by either infinite series or closed-form expressions, and the sums of these infinite series over the blade index also have closed-form representations. Hence, symbolic functions are available representing an elemental ring representing blades acting in concert (as an entity). These functions may also be expressed by either infinite series or closed-form expressions. In addition, it is shown that an evaluation at some radial station on a blade is representative of the normalized radial integral over the entire blade. Hence, an elemental ring may be generalized to the entire rotor disc. These important relationships permit the symbolic representation of the orientation of an entire rotor disc (as well as all of its vibration modes) as either an infinite series or a closed-form expression. Finally, at the disc level of modeling the required additions are reduced to very simple mathematical relationships. By retaining multiple harmonic relationships until the final point of approximation, PROMO is shown to yield accurate N/rev distortions of the rotor disc. This is in contrast to typical, low-order Fourier representations that cannot possibly produce high order harmonics.

Inaccuracies of numerical integration algorithms operating on high frequency (blade level) variables in RBEs are avoided in PROMO by relegating integration processes to slowly varying variables such as those describing the gross behavior of the rotor disc, while creating a rotor system's high frequency content using known generating functions, or kernels. These generating functions deliver harmonic spectra that are representative of those from nonlinear, blade-element models, and they can be calibrated to deliver the appropriate *N*/rev power level at all flight speeds. PROMO may be computed at the component level or "as a system," for application to any TPP model. Its availability should impact rotor research in such topics such as rotor turbulence modeling and harmonic control. For a rotor disc model, the simplified, approximate form of PROMO emulates the N/rev harmonic of a distributed rotor model, without the undesirable feature of RBEs that alias undesirable high-order harmonics into a pilot's operational bandwidth.

2.0 Definitions

Fourier series representations of periodic functions may be used for the specification and distribution of harmonic frequencies. Truncated to the first harmonic, such representations are used in TPP rotor models to represent the sinusoidal flapping motion of individual blades. The independent variable is typically the blade's azimuth angle "ψ," measured counterclockwise from aft in the rotor plane. However, considering an arbitrary advance ratio, this purely mathematical construct belies the fact that a blade's observed periodicity has its origin firmly based in the physics of rotary motion while translating through an air mass (or velocity field). This phenomenon is more concisely represented when the independent variable is changed to be the primary rotational variable that actually produces the asymmetric aerodynamics, here called the "advance angle λ." It has a 90-degree bias from a blade's "azimuth angle" and is measured in the wind axes rather than in the body axes. This change in representation is motivated by the fact that the "study of swept wing aerodynamics has shown that the component of velocity perpendicular to the leading edge is the only velocity that is important in establishing aerodynamic forces."[8] Furthermore, "neglecting radial flow is an acceptable assumption." These facts are used here in combination with the fact that the collective and cyclic controls in TPPs establish the low-frequency orientation of a rotor disc. Hence, the basic physics of blade flapping are revealed by PROMO through some elementary assumptions.

The "azimuth angle ψ_n" of an individual blade ($n = 1,2...,N$) of a rotor system with *"N"* equally spaced blades may be represented in terms of the azimuth angle of just one "master" blade (where *n*=1). The blade's azimuth angle is related to that of the master blade ($\psi = \psi_1$) by,

$$\psi_n = \psi + \frac{2\pi(n-1)}{N} \tag{2.1}$$

The time integral of the rotor system RPM (not necessarily constant) may then be conveniently defined as the azimuth angle of the master blade.

[8] Helicopter Performance, Stability, and Control, Raymond W. Prouty, Robert E. Krieger Publishing Co., Malabar, FL 1990, p. 141

$$\psi = \psi_1 = \int \Omega dt \tag{2.2}$$

The "advance angle" of a given blade, rather than the azimuth angle, is related to both the azimuth angle of that blade and the vehicle velocity vector. Considering the aerodynamic sideslip angle β_w, the n^{th} blade's "advance angle" (with respect to the rotor-plane vehicle velocity) is then related to the "azimuth angle" by,

$$\lambda_n = \psi_n - \beta_w + \pi/2 \tag{2.3}$$

The variable λ (without subscript) represents the "master," or first blade. The "master blade" is identified in Fig. 1 with its azimuth angle ψ with respect to the vehicle's aft longitudinal axis. For this blade the azimuth angle and the blade advance angle need not be displayed with the index "l". Blades 2, 3 and 4 follow consecutively, and are referred to by the advance angles λ_n ($n = 1,2,...,N$).

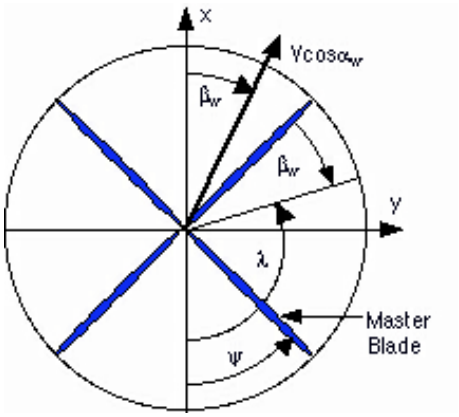

Fig. 1 – Velocity and Blade Angles

Hence, the advance angle for any blade may be written in terms of the advance angle for the master blade.

$$\lambda_n = \lambda_1 + \frac{2\pi(n-1)}{N} = \psi_1 - \beta_n + \frac{\pi}{2} + \frac{2\pi(n-1)}{N} \tag{2.4}$$

In Fig. 1, notice that λ_n is measured from the aft vehicle axis, just as is ψ_n. Sans sideslip this angle is 90 degrees greater than a blade's azimuth angle (with respect to the vehicle's aft centerline). Since this denotes a functionality perpendicular to, rather than parallel to a blade's tangential velocity, aerodynamic relationships are more concisely expressed, and produce rather elegant representations as functions of Poisson's kernel.

3.0 Poisson's Kernel

Assuming geometrically decreasing positive coefficients, infinite series may be created using the advance angle, without the artifice of introducing degrees of freedom such as "reactionless modes".[9] The selected series are members of mathematical constructs called "generating functions," and in particular, a classic generating function called "Poisson's kernel". Because of the assumed geometric series structure of the coefficients, the infinite series representation does not require the use of any more parameters than conventional trigonometric representations (that are truncated to the first harmonic). Indeed, for hovering flight the representation actually collapses to that of the conventional sine and cosine representation. The geometric series structure is that which creates harmonics replicating those created by blade-element

[9] Helicopter Theory, Wayne Johnson, Princeton University Press, Princeton, NJ, 1980, p. 351

models for harmonics at least out to *N*/rev. At the blade level of modeling these harmonics closely match those of RBEs, and most importantly, at the disc level of modeling, this means that the harmonic selection (see Appendix A) that occurs under summation in RBEs is duplicated by PROMO, *i.e.,* it creates multi-axis N/rev harmonics properly phased and related to the orientation of the rotor plane.

The Poisson model permits both the summation and resolution of individual blade flapping contributions to the rotorcraft axes. This is required to produce closed-form expressions for rotor forces and moments. Spectral filtering occurs under summation over the number of blades, such that only harmonics that are multiples of the number of blades survive (for blades with identical physical properties). The equivalent series representations may be truncated to any number of terms for diverse purposes such as eliminating aliasing or determining the influence of modal forms.

For hovering rotorcraft the periodic trajectories of the individual rotor blade flapping angles manifest the distinct frequency content of the rotor system RPM "Ω," plus any non-periodic, commanded collective and cyclic control frequencies. Near the hover condition the higher harmonics are negligible, and for a system of blades with identical physical properties they vanish. However, as the vehicle gains rotor-plane aerodynamic velocity, the blades experience an increasingly asymmetric velocity field, and harmonics of the RPM are excited for each blade as a function of advance and swash plate angles. These harmonics represent nonlinear variations in the angle of attack on a blade, and are a function of the advance ratio at a given radial station. With an in-plane aerodynamic velocity "*V*," at a distance "*r*" from the rotor hub the "advance ratio" is typically defined as $\mu = V/\Omega r$. This will later be redefined.

Individual rotor blades exhibit considerable periodic behavior. Therefore, mathematical representations of blade variables such as flapping angles are often given as harmonic series, where for practical reasons these series are truncated to a low number of terms. While truncating these series has little influence in the representation of individual blade motion at hover, at any significant velocity the high order harmonics are invariably lost. This loss is not very perceptible at the blade element level of modeling. However, for any significant vehicle velocity the N/rev harmonic becomes significant under blade summation, such as is required when creating total rotor forces and moments. For higher-order representations such as RBE models, the pertinent variables, when summed over the number of blades (*N*), exhibit spectral filtering of all harmonic content save that which is a multiple of the number of blades. Hence, accurate mathematical representations of blade variables must contain at least "*N*" harmonic terms if the fundamental frequency content is to be preserved under summation over the blade index. This *N*/rev phenomenon[10] occurs in a rotor system as the individual blades track each other.

Additionally, typical Fourier representations of blade dynamics[11] are not optimum because they utilize the azimuth angle variable, rather than the advance angle, an angular variable closely associated with the aerodynamics of a rotor system. The fascinating functions that utilize this variable are analyzed here, and for the rotor system as a disc plane, considerable simplifications are developed.

For harmonic representations of flapping angles, the low-order parameters such as collective, longitudinal and lateral cyclic (a_0, a_1, a_2) are well known, and the low order trigonometric representation for blade variables is useful, resulting in the mean collective and cyclic angles (A_{0F}, A_{1F}, B_{1F}). However, the properties of the mathematical formulation known as "Poisson's kernel" present compelling reasons for expressing blade variables as infinite harmonic series with geometrically decreasing coefficients. They replicate the first few harmonics of the spectra of nonlinear models very well, and they additionally have closed-form representations. These harmonic representations do not use the blade azimuth angle as the independent variable, but rather, an angle that is 90-degrees advanced from a blade's azimuth angle with respect to the wind vector, here called the advance angle. This representation is a natural consequence of the physics of rotary motion in a velocity field, and yields tractable, non-alternating, monotonically decreasing sine and cosine series. Where a normalized "Poisson parameter" is defined as "ρ," for $0 \le \rho < 1$ two trigonometric series of interest converge to the following simple expressions,

---

[10] The N/Rev Phenomenon in Simulating a Blade-Element Rotor System, R. E. McFarland, NASA TM 84344, March, 1983

[11] Effects of Primary Rotor Parameters on Flapping Dynamics, Robert T. N. Chen, NASA TP 1431, 1980, p. 25.

$$\sum_{k\geq 1} \rho^{k-1} \cos k\lambda \;=\; \frac{\cos\lambda - \rho}{1 - 2\rho\cos\lambda + \rho^2}$$
$$\sum_{k\geq 1} \rho^{k-1} \sin k\lambda \;=\; \frac{\sin\lambda}{1 - 2\rho\cos\lambda + \rho^2} \qquad (3.1)$$

With an appropriate definition for ρ, one advantage of these expressions is that their denominators contain a representation of the dynamics of a blade's tangential velocity. Tangential velocity generally appears in the denominators of expressions for angles of attack, and by implication, significantly contribute to flapping and lagging angles. These are the primary functionalities that generate harmonics in a rotor system. Other advantages accrue from using these relationships, especially when all of the blades of a rotor system are considered.

4.0 Radial Element Locations

The Black Hawk rotor system is used for comparison purposes and for calibration. Its rotor system has four blades (*N*=4) and for each of the blades the number of segments used in simulation is typically five (*M*=5), at least at Ames Research Center. Blades are defined by ($1 \le n \le N$), and segments by ($1 \le m \le M$). In the Black Hawk blade-element model the "equal annuli" algorithm is generally used to compute the radial distances to the blade elements.

$$r_m = \sqrt{(e+e')^2 + \left(\frac{m-1/2}{M}\right)\left[R^2 - (e+e')^2\right]} - e \qquad (4.1)$$

The rotor radius is *R*=26.83 ft, the hinge offset is e=1.25 ft, and the spar length is e'=2.25 ft.

The equal annuli algorithm distributes the radii of evaluation to positions where their associated lengths or "segments" (under summation) tend to have similar loads. It may be said that the more radii that are used, the more accurate the result. However, for the computation of flapping angles this is certainly not the case, especially if any evaluation radius is near the stall region. This difference occurs because each (stiff) blade has only one instantaneous flapping angle independent of radius, while direct computations for angles of attack vary wildly for radii near a stall region. RBEs avoid the mathematical problem at radial stations near stall by decreasing the angle of attack contribution to blade forces via nonlinear operations involving decreases in dynamic pressure. In an RBE the flapping angle for a blade is computed from summed forces and moments, which are evaluated using distinct angles of attack and dynamic pressure, and integrated. For the PROMO model the problem is avoided by noting that summed radial values of the kernel differ negligibly from evaluations at a single radial point well displaced from any stall region. Since simplified rotor models generally avoid evaluations near regions of reverse flow, the Poisson model developed here is no exception. Furthermore, the stall region does not contribute much to flapping despite divergent angles of attack. Hence, for the computation of flapping angles the radial evaluation criterion is not as stringent as might be assumed, and a single evaluation point somewhere on a blade is generally sufficient. After these points are demonstrated, the radial functionality for the Poisson parameter is itself eliminated. The Poisson parameter becomes a function of only the flight speed.

5.0 Tangential Velocity

In PROMO a blade's tangential velocity is expressed using its "advance angle" rather than its azimuth angle. "Ω" is the angular rate (or RPM) of the rotor system in rad/sec, and "$V\cos\alpha_w$" is the rotor in-plane or horizontal velocity of the vehicle with respect to the air mass, in ft/sec. The tangential velocity "*v*" at a radial element at radius "*r*" is then given by,

$$v \;=\; \Omega r + V\cos\alpha_w \sin(\psi - \beta_w) \;=\; \Omega r + V\cos\alpha_w \sin\left(\lambda - \frac{\pi}{2}\right) \;=\; \Omega r\left(1 - \frac{V\cos\alpha_w}{\Omega r}\cos\lambda\right) \qquad (5.1)$$

The advance ratio "μ" is typically defined as the coefficient of $\cos\lambda$ in the above equation. It appropriately vanishes at hover when *V*=0. μ approaches unity when the rotor plane aerodynamic velocity approaches the rotational velocity at

the particular radial element ($V\cos\alpha_w = \Omega r$). This would produce stall on the retreating blades. As rotorcraft velocity increases, the condition of stall occurs first in an RBE model when the inboard element "r_1" has a tangential velocity that vanishes at the advance angle of exactly 360 degrees (not azimuth angle, which would be about 270 degrees). Computations near stall are avoided by selecting only one relatively large radial station. Consider then, that the advance ratio "μ" at some radius is related to the advance variable "ρ" from Poisson's kernel by the relationships:

$$\begin{aligned} \mu &= \frac{V\cos\alpha_w}{\Omega r} = \frac{2\rho}{1+\rho^2} \\ \rho &= \frac{\Omega r}{V\cos\alpha_w} - \sqrt{\left(\frac{\Omega r}{V\cos\alpha_w}\right)^2 - 1} = \frac{1-\sqrt{1-\mu^2}}{\mu} \end{aligned} \tag{5.2}$$

The closed form expressions for the infinite series of Equation (3.1) are then recognized as containing denominators proportional to an element's tangential velocity, *i.e.*,

$$v = \Omega r\left(1 - \mu\cos\lambda\right) \tag{5.3}$$

The infinite series from Poisson's kernel may therefore be written so that their closed-form equivalents have denominators that are functions of the blade's tangential velocity. For individual blades, the following harmonic series then become useful in the expression of a flapping angle. For $0 \le \rho < 1$, the two trigonometric series for the n^{th} blade are,

$$\begin{aligned} s_n &= \sum_{k\ge 1} \rho^{k-1}\sin\left(k\lambda_n\right) = \frac{\sin\lambda_n}{1+\rho^2-2\rho\cos\lambda_n} \\ c_n &= \sum_{k\ge 1} \rho^{k-1}\cos\left(k\lambda_n\right) = \frac{\cos\lambda_n - \rho}{1+\rho^2-2\rho\cos\lambda_n} \end{aligned} \tag{5.4}$$

By using the advance angle λ_n rather than the azimuth angle ψ_n, the infinite series coefficients do not have alternating signs. They are simple power series of a single variable, and the blade closed-form solutions contain denominators that are functions of the tangential velocity of the particular blade. Note that strictly speaking the inverse of the tangential velocity should be used to express a blade's angle of attack, rather than the flapping angle. However, the assumption is made that functional relationships and data do not exist to connect the angles of attack to flapping angles. Hence, tuning will be required, and it will involve power relationships rather than functions of tangential velocity.

6.0 Radial Evaluation

The characteristics of blade-level variables change with variations in advance ratio, and advance ratio is a function of velocity and radial distance. For example, consider the first (master) blade, and the series presented above. If $\mu = 0$ (such that $\rho = 0$) these collapse to a sine and cosine function, as indicated in Fig. 2(a). However, if some huge value $\mu = 0.8$ (such that $\rho = 0.5$) is used, the series would become highly nonlinear, as indicated in Fig. 2(b).

Richard McFarland
Comment: betansc.igr, betansc.PICT

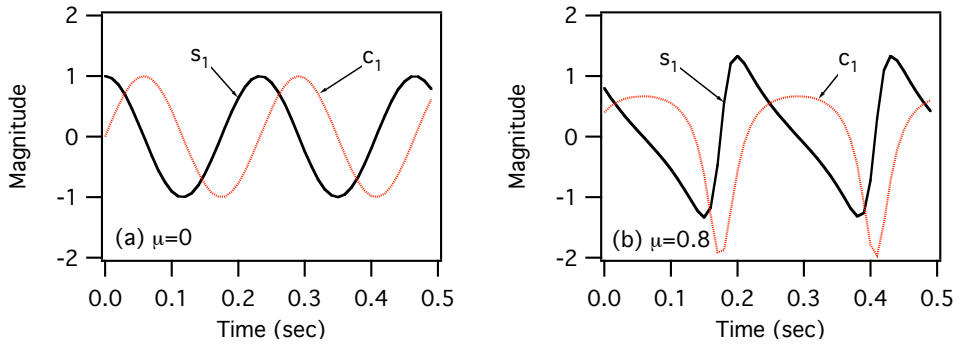

Fig. 2 – Flapping Component Changes with Advance Ratio

The actual Poisson parameter is later shown to never approach such a large value as one-half. Fig. 2 is simply useful to show that a blade's flapping angle becomes nonlinear with significant advance ratio.

Flapping (or lagging) angles may be expressed in terms of the above trigonometric series (s_n, c_n). Before they are introduced, however, consider how accurately radial evaluations represent the integral over a blade. Using the Equal Annuli Algorithm of Equation 4.1, stall occurs initially with increasing velocity on the first (interior) segment (m=1). Stall could be avoided by limiting the velocity, as a function of the number of segments according to the following graph.

Richard McFarland
Comment: Poisson:radius.pict from radius.vi and stall.igr

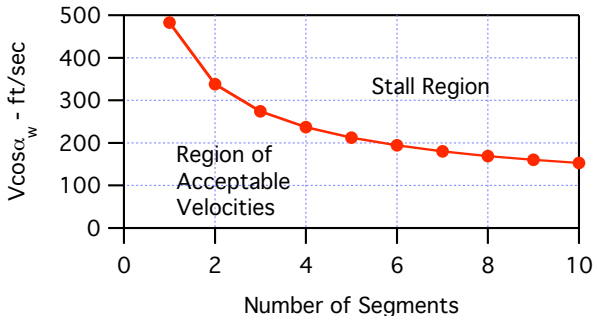

Fig. 3 – Stall Boundary (Equal Annuli Algorithm)

This limitation is annoying because the interior evaluation radius produces the stall phenomenon at relatively low velocities when many evaluation radii are used; this is counterproductive. In PROMO stall is necessarily avoided in the computation of flapping. The model therefore accommodates very high vehicle velocities of which the advance ratio becomes a function.

To a very good approximation, there exists an optimum radius for evaluating the trigonometric functions (s_n, c_n) and hence the flapping angles. This radius may be found by examining the normalized integrals of the trigonometric functions over radius, where the evaluation points are those given by the Equal Annuli Algorithm. The normalized integrals using the equal-annuli radii limits are given by the following expressions,

$$
\begin{aligned}
I_s(n) &= \frac{1}{(r_M - r_1)}\int_{r_1}^{r_M} s_n\,dr = \frac{V\cos\alpha_w \sin\lambda_n}{2\Omega(r_M - r_1)}\int_{\rho_1}^{\rho_M}\frac{(1-\rho^{-2})\,d\rho}{1+\rho^2 - 2\rho\cos\lambda_n} \\
&= \frac{V\cos\alpha_w \sin\lambda_n}{2\Omega(r_M - r_1)}\left\{2\sin\lambda_n\left[\tan^{-1}\left(\frac{\rho_M - \cos\lambda_n}{\sin\lambda_n}\right) - \tan^{-1}\left(\frac{\rho_1 - \cos\lambda_n}{\sin\lambda_n}\right)\right]\right. \\
&\left. + \frac{1}{\rho_M} - \frac{1}{\rho_1} + \cos\lambda_n \ln\left[\frac{\rho_1^2(1+\rho_M^2 - 2\rho_M\cos\lambda_n)}{\rho_M^2(1+\rho_1^2 - 2\rho_1\cos\lambda_n)}\right]\right\}
\end{aligned}
\tag{6.1}
$$

$$
\begin{aligned}
I_c(n) &= \frac{1}{(r_M - r_1)}\int_{r_1}^{r_M} c_n\,dr = \frac{V\cos\alpha_w}{2\Omega(r_M - r_1)}\int_{\rho_1}^{\rho_M}\frac{(1-\rho^{-2})(\cos\lambda_n - \rho)\,d\rho}{1+\rho^2 - 2\rho\cos\lambda_n} \\
&= \frac{V\cos\alpha_w}{2\Omega(r_M - r_1)}\left\{2\sin\lambda_n\cos\lambda_n\left[\tan^{-1}\left(\frac{\rho_M - \cos\lambda_n}{\sin\lambda_n}\right) - \tan^{-1}\left(\frac{\rho_1 - \cos\lambda_n}{\sin\lambda_n}\right)\right]\right. \\
&\left. + \cos^2\lambda_n \ln\left[\frac{\rho_1^2(1+\rho_M^2 - 2\rho_M\cos\lambda_n)}{\rho_M^2(1+\rho_1^2 - 2\rho_1\cos\lambda_n)}\right] + \frac{\cos\lambda_n}{\rho_M} - \frac{\cos\lambda_n}{\rho_1} + \ln\left[\frac{\rho_M(1+\rho_1^2 - 2\rho_1\cos\lambda_n)}{\rho_1(1+\rho_M^2 - 2\rho_M\cos\lambda_n)}\right]\right\}
\end{aligned}
\tag{6.2}
$$

Hence, closed-form expressions exist for the normalized integral of the trigonometric functions over the effective blade length. The integrals represent components of the average instantaneous flapping angle for that blade at that advance angle. The summed evaluations of the trigonometric series over the blade radii are also good representations of these integrals. For example, a midpoint evaluation technique may be used to compute the normalized sums:

$$
\begin{aligned}
J_s(n) &= \frac{1}{(r_M - r_1)}\sum_{m=1}^{M} s_n(r_m)\Delta r \approx \frac{1}{2(r_M - r_1)}\sum_{m=1}^{M-1}\left[s_n(r_{m+1}) + s_n(r_m)\right]\left[r_{m+1} - r_m\right] \\
J_c(n) &= \frac{1}{(r_M - r_1)}\sum_{m=1}^{M} c_n(r_m)\Delta r \approx \frac{1}{2(r_M - r_1)}\sum_{m=1}^{M-1}\left[c_n(r_{m+1}) + c_n(r_m)\right]\left[r_{m+1} - r_m\right]
\end{aligned}
\tag{6.3}
$$

These normalized sums should closely approximate the closed-form radial integrals given above, *i.e.*,

$$
\begin{aligned}
J_s(n) &\approx I_s(n) = \frac{1}{2(r_M - r_1)}\int_{r_1}^{r_M} s_n(r)\,dr \\
J_c(n) &\approx I_c(n) = \frac{1}{2(r_M - r_1)}\int_{r_1}^{r_M} c_n(r)\,dr
\end{aligned}
\tag{6.4}
$$

This comparison leads to the fact that some radius r_a may be used to evaluate the trigonometric series (s_n and c_n), and the evaluation will then approximate the normalized integral (I_s or I_c) to a high degree of accuracy. Because the flapping angle will be shown to be a function of I_s and I_c (and hence s_n and c_n), this permits the computation of flapping by using just a single radial evaluation point, r_a. That is, the normalized integrals over the blade's radius (at a given velocity) equal the integrand evaluated at some radius r_a (where the Poisson parameter is ρ_a):

$$
\begin{aligned}
s_n(r_a) &= \frac{\sin\lambda_n}{1+\rho_a^2 - 2\rho_a\cos\lambda_n} \cong I_s(n) = \frac{1}{r_M - r_1}\int_{r_1}^{r_M} s_n(r)\,dr \\
c_n(r_a) &= \frac{\cos\lambda_n - \rho_a}{1+\rho_a^2 - 2\rho_a\cos\lambda_n} \cong I_c(n) = \frac{1}{r_M - r_1}\int_{r_1}^{r_M} c_n(r)\,dr
\end{aligned}
\tag{6.5}
$$

Combining these expressions at a given velocity and azimuth angle, the value for ρ_a may be computed.

$$\rho_a = \cos\lambda_n - \frac{I_c(n)}{I_s(n)}\sin\lambda_n \tag{6.6}$$

The optimum radius r_a for evaluation would then be given by,

$$r_a = \frac{V\cos\alpha_w\left(1+\rho_a^2\right)}{2\Omega\rho_a} \tag{6.7}$$

This radius r_a is a function of velocity as well as advance angle, as shown in Fig. 4. In this figure the advance angle makes two complete revolutions and the velocity ranges from zero up to 200 ft/sec in 20 ft/sec increments.

Richard McFarland
Comment: poisson:drsc.vi:optR.pict

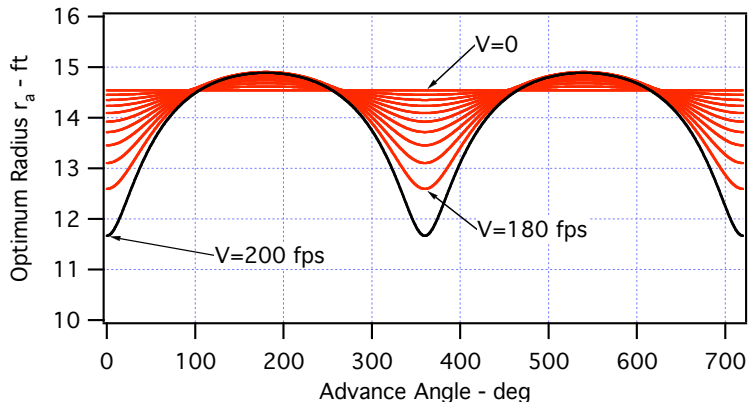

Fig. 4 – Optimum Radius

Hence, the optimum radius to use for substitution into the Poisson sine or cosine series as an approximation to its integral over the radius may be evaluated. The radius then delivers values for s_n and c_n that closely approximate I_s and I_c. From Fig. 4 the lower the velocity, the less the radius influences the trigonometric terms. A large velocity is therefore used in Fig. 5 where this phenomenon is displayed. The results are shown to be not very sensitive to the radius of evaluation. For instance, the arbitrary radius of $r_a = R/2 = 13.415$ ft produces good approximations for I_s and I_c for all velocities. Using a high velocity of 200 ft/sec, the normalized integrals of s_n and c_n are nearly coincident with their non-integrated evaluations at $r_a = R/2$ ft at all advance angles. This is illustrated in Fig. 5.

Richard McFarland
Comment: drsc.igr

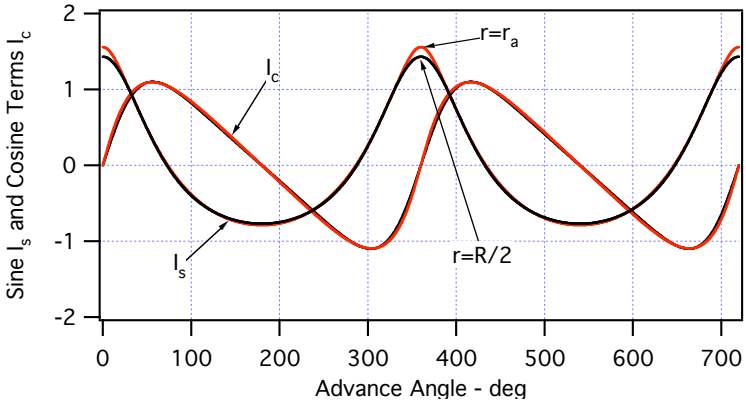

Fig. 5 – Sine and Cosine Series at *V*=200 ft/sec

Approximations become more accurate for lower velocities, so simple integrand evaluations at constant radii generally represent normalized integrals over a blade. The trigonometric terms do not vary much for the complete velocity range. For the range of velocities up to 200 ft/sec in 20 ft/sec increments the closed-form integrals are shown in Fig. 6.

Richard McFarland
Comment: poisson:drsc.vi:drsc.igr:drsc1.pic t

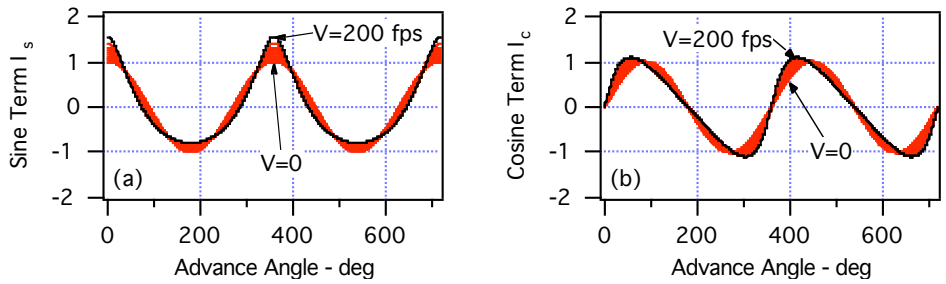

Fig. 6 – Integrated Series

Very similar results are obtained using a single evaluation radius. In Fig. 7 the sine and cosine series evaluations are used at the half radius, rather than the integrals of Fig. 6. When the half-radius is used, the trigonometric sums are almost identical over a wide range of vehicle velocities.

Richard McFarland
Comment: drsc/igr

Richard McFarland
Comment: poisson.drsc.vi:drsc.igr:drsc2.pic t

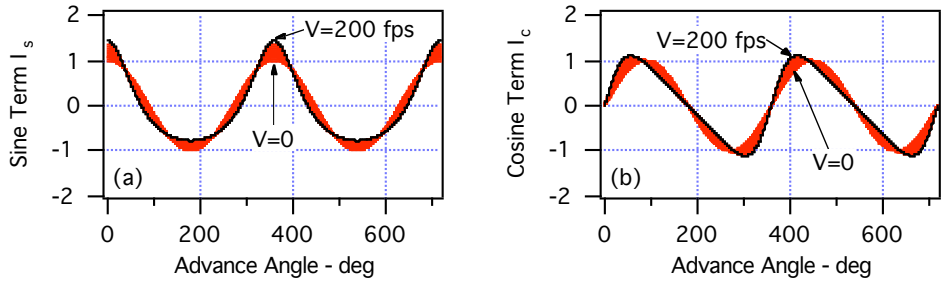

Fig. 7 – Non-integrated Series Evaluated at *R/2*

Since similar results are obtained for all velocities, for all practical purposes an evaluation at some radius is equivalent to radial integration.

$$\begin{aligned} s_n(r_a) &= I_s(n) \\ c_n(r_a) &= I_c(n) \end{aligned} \tag{6.8}$$

This replacement is possible because evaluations of the trigonometric series are generally insensitive to the radius of evaluation. An additional summation over the blade index then becomes possible, such that the entire orientation of the rotor disc may be expressed by either the infinite series or closed-form solutions of Poisson's kernel. This is shown in Section 7.0.

The insensitivity of the Poisson representation to radius suggests that the Poisson parameter must generally be very small, and that it should be evaluated differently than by radial evaluation. However, the mathematical form should be preserved. Such a technique is derived below, where the Poisson parameter is determined by the simple requirement of delivering accurate spectral power at N/rev.

7.0 Summations Over the Blade Index

The two series based upon Poisson's kernel as summed over the blade index result in either closed-form expressions or infinite series, which are components of mathematical expressions for flapping. Appendix A describes certain mathematical operations required to compute the series summations. The summations over the blade index for s_n and c_n are,

$$\begin{aligned} S &= \frac{1}{N}\sum_{n=1}^{N}\sum_{k=1}^{\infty}\rho^{k-1}\sin(k\lambda_n) = \frac{1}{\rho N}\sum_{m=1}^{\infty}\rho^{m}\sum_{n=1}^{N}\sin(m\lambda_n) = \sum_{k=1}^{\infty}\rho^{kN-1}\sin(kN\lambda) = \frac{\rho^{N-1}\sin(N\lambda)}{1-2\rho^{N}\cos(N\lambda)+\rho^{2N}} \\ C &= \frac{1}{N}\sum_{n=1}^{N}\sum_{k=1}^{\infty}\rho^{k-1}\cos(k\lambda_n) = \frac{1}{\rho N}\sum_{m=1}^{\infty}\rho^{m}\sum_{n=1}^{N}\cos(m\lambda_n) = \sum_{k=1}^{\infty}\rho^{kN-1}\cos(kN\lambda) = \frac{\rho^{N-1}\left[\cos(N\lambda)-\rho^{N}\right]}{1-2\rho^{N}\cos(N\lambda)+\rho^{2N}} \end{aligned} \tag{7.1}$$

Notice the spectral filtering that occurs when the trigonometric series are summed over the blade index. Only multiples of *N*/rev survive.

8.0 Flapping Angles

Finally, the flapping angles are addressed. The flapping angles and even the derivatives of flapping angles may be written as functions of the Poisson generating functions,

$$\begin{aligned}
\beta_n &= a_0 - a_1 s_n + a_2 c_n \\
\dot{\beta}_n &= \dot{a}_0 - \dot{a}_1 s_n + \dot{a}_2 c_n - a_1 \dot{s}_n + a_2 \dot{c}_n \\
\ddot{\beta}_n &= \ddot{a}_0 - \ddot{a}_1 s_n + \ddot{a}_2 c_n + 2\left(\dot{a}_2 \dot{c}_n - \dot{a}_1 \dot{s}_n\right) - a_1 \ddot{s}_n + a_2 \ddot{c}_n
\end{aligned} \tag{8.1}$$

If the advance ratio μ (or the Poisson parameter ρ) vanishes, the infinite series are reduced to only one term, so that for negligible sideslip and control activity the flapping variables become familiar expressions,

$$\begin{aligned}
\beta_n &= a_0 - a_1 \sin\lambda_n + a_2 \cos\lambda_n \approx a_0 - a_1 \cos\psi_n - a_2 \sin\psi_n \\
\dot{\beta}_n &= -\Omega\left(a_2 \sin\lambda_n + a_1 \cos\lambda_n\right) \approx \Omega\left(a_1 \sin\psi_n - a_2 \cos\psi_n\right) \\
\ddot{\beta}_n &= \Omega^2\left(a_1 \sin\lambda_n - a_2 \cos\lambda_n\right) \approx \Omega^2\left(a_1 \cos\psi_n + a_2 \sin\psi_n\right)
\end{aligned} \tag{8.2}$$

These relationships are consistent with the definitions for collective, longitudinal and lateral cyclic. For a rotor system with four blades, at cardinal azimuth locations the flapping angles are,

$$\begin{aligned}
\beta_{\lambda_c=0}\left(\psi_n \approx \frac{3\pi}{2}\right) &= a_0 + \frac{a_2}{1-\rho} \quad \underset{\rho\to 0}{\Rightarrow} \quad a_0 + a_2 \\
\beta_{\lambda_c=\frac{\pi}{2}}\left(\psi_n \approx 0\right) &= a_0 - \frac{a_1 + a_2\rho}{1+\rho^2} \quad \underset{\rho\to 0}{\Rightarrow} \quad a_0 - a_1 \\
\beta_{\lambda_c=\pi}\left(\psi_n \approx \frac{\pi}{2}\right) &= a_0 - \frac{a_2}{1+\rho} \quad \underset{\rho\to 0}{\Rightarrow} \quad a_0 - a_2 \\
\beta_{\lambda_c=\frac{3\pi}{2}}\left(\psi_n \approx \pi\right) &= a_0 + \frac{a_1 - a_2\rho}{1+\rho^2} \quad \underset{\rho\to 0}{\Rightarrow} \quad a_0 + a_1
\end{aligned} \tag{8.3}$$

These are also consistent with traditional formulations. It is also of interest to see the infinite series for flapping in terms of azimuth angle. In this case, when sideslip is zero, the expansion is given by,

$$\begin{aligned}
\beta_n = a_0 &- a_1\left[\cos\psi_n - \rho\sin 2\psi_n - \rho^2\cos 3\psi_n + \rho^3\sin 4\psi_n + \ldots\right] \\
&- a_2\left[\sin\psi_n + \rho\cos 2\psi_n - \rho^2\sin 3\psi_n - \rho^3\cos 4\psi_n + \ldots\right]
\end{aligned} \tag{8.4}$$

Therefore, the alternating forms of these series are more complicated than the selected form that uses the advance angle. Both the signs and the form of the trigonometric expressions are much simplified.

9.0 Tip Path Plane Considerations

In this derivation the orientation of the tip path plane has been assumed known. This may be accomplished via a variety of techniques. For example, the swash plate angles are usually computed[12] from typical elevator, aileron and collective inputs ($\delta_e, \delta_a, \delta_c$) such as,

$$\begin{aligned}
A_{1c} &= C_1\delta_a + C_3\delta_e + C_{A_{\lambda_c}} \\
B_{1c} &= C_2\delta_a + C_4\delta_e + C_{B_{\lambda_c}} \\
\theta_0 &= C_6\delta_c + C_5
\end{aligned} \tag{9.1}$$

[12] A Mathematical Model of a Single Main Rotor Helicopter for Pilot Simulation, Peter D. Talbot, Bruce E. Tinling, William A. Decker, and Robert T. N. Chen, NASA TM 84281, Sept. 1982

Cross coupling is required when controls are related to the azimuth angle rather than the advance angle. These terms probably vanish using PROMO. That is, the cyclic controls may be uncoupled by using the advance angle. PROMO also has the feature that it does not require the transformation to the wind axes,

$$\begin{aligned} A_{1s} &= A_{1c}\cos\beta_w - B_{1c}\sin\beta_w \\ B_{1s} &= A_{1c}\sin\beta_w + B_{1c}\cos\beta_w \end{aligned} \tag{9.2}$$

The mathematical representation is already in the wind axis system so that $A_{1s} = A_{1c}$ and $B_{1s} = B_{1c}$. The coefficients used in the derivation are then given by,

$$\begin{aligned} a_0 &= \theta_0 \\ a_1 &= A_{1s} \\ a_2 &= B_{1s} \end{aligned} \tag{9.3}$$

There may be some representative dynamics[13] between the control deflections and the swash plate response, such as,

$$\begin{aligned} a_1(s) &= A_{1s}(s) = \frac{A_{1c}}{\tau_R s + 1} \\ a_2(s) &= B_{1s}(s) = \frac{B_{1c}}{\tau_R s + 1} \end{aligned} \tag{9.4}$$

10.0 Summed Flapping Angles

The collective and cyclic angles are functions of the flapping angles. To express certain required functions of flapping and lagging angles it is convenient to have the summation of the following resolved series:

$$S_a = \frac{2}{N}\sum_{n=1}^{N}\sum_{k\geq 1}\rho^{k-1}\sin(k\lambda_n)\sin(\lambda_n) = 1 + \left(\rho - \frac{1}{\rho}\right)C \tag{10.1}$$

$$C_a = \frac{2}{N}\sum_{n=1}^{N}\sum_{k\geq 1}\rho^{k-1}\cos(k\lambda_n)\sin(\lambda_n) = \left(\frac{1}{\rho} - \rho\right)S \tag{10.2}$$

$$S_b = \frac{2}{N}\sum_{n=1}^{N}\sum_{k\geq 1}\rho^{k-1}\sin(k\lambda_n)\cos(\lambda_n) = \left(\rho + \frac{1}{\rho}\right)S \tag{10.3}$$

$$C_b = \frac{2}{N}\sum_{n=1}^{N}\sum_{k\geq 1}\rho^{k-1}\cos(k\lambda_n)\cos(\lambda_n) = 1 + \left(\rho + \frac{1}{\rho}\right)C \tag{10.4}$$

$$\frac{2}{N}\sum_{n=1}^{N}\beta_n\sin\lambda_n = -a_1\left[1 + \left(\rho - \frac{1}{\rho}\right)C\right] + a_2\left(\frac{1}{\rho} - \rho\right)S = -a_1 S_a + a_2 C_a \tag{10.5}$$

---

[13] A Mathematical Force and Moment Model of a UH-1H Helicopter for Flight Dynamics Simulations," Peter D. Talbot and Lloyd D. Corliss, NASA TM-73-254, June 1977

$$\frac{2}{N}\sum_{n=1}^{N}\beta_n\cos\lambda_n = -a_1\left(\rho+\frac{1}{\rho}\right)S + a_2\left[1+\left(\rho+\frac{1}{\rho}\right)C\right] = -a_1S_b + a_2C_b \tag{10.6}$$

The collective, longitudinal and lateral cyclic angles are then given by,

$$A_{0F} = \frac{1}{N}\sum_{n=1}^{N}\beta_n = a_0 - a_1S + a_2C \tag{10.7}$$

$$\begin{aligned} A_{1F} &= -\frac{2}{N}\sum_{n=1}^{N}\beta_n\cos\psi_n = -\frac{2}{N}\sum_{n=1}^{N}\beta_n\sin\left(\psi_n+\frac{\pi}{2}\right) \\ &= -\frac{2}{N}\sum_{n=1}^{N}\beta_n\sin\left(\lambda_n+\beta_w\right) = -\frac{2}{N}\sin\beta_w\sum_{n=1}^{N}\beta_n\cos\lambda_n - \frac{2}{N}\cos\beta_w\sum_{n=1}^{N}\beta_n\sin\lambda_n \\ &= \left(a_1S_b - a_2C_b\right)\sin\beta_w - \left(-a_1S_a + a_2C_a\right)\cos\beta_w \end{aligned} \tag{10.8}$$

$$\begin{aligned} B_{1F} &= -\frac{2}{N}\sum_{n=1}^{N}\beta_n\sin\psi_n = \frac{2}{N}\sum_{n=1}^{N}\beta_n\cos\left(\psi_n+\frac{\pi}{2}\right) \\ &= \frac{2}{N}\sum_{n=1}^{N}\beta_n\cos\left(\lambda_n+\beta_w\right) = \frac{2}{N}\cos\beta_w\sum_{n=1}^{N}\beta_n\cos\lambda_n - \frac{2}{N}\sin\beta_w\sum_{n=1}^{N}\beta_n\sin\lambda_n \\ &= \left(a_1S_a - a_2C_a\right)\sin\beta_w + \left(-a_1S_b + a_2C_b\right)\cos\beta_w \end{aligned} \tag{10.9}$$

11.0 Poisson Parameter

RBE models compute angles of attack for each segment, which are used for table lookups to create blade forces and moments. Along with flapping and lagging states of each blade, these variables are used as forcing functions in nonlinear differential equations representing flapping and lagging accelerations, which are then integrated. Summations are then performed to determine the orientation of the rotor as a disc. In a TPP model the orientation of the rotor disc is otherwise determined, and this orientation is used to determine the rotor system's forces and moments. Hence, in PROMO an individual blade's efficiency is immaterial in the representation of flapping angles, although the fundamental physical relationships are retained.

By changing the definition of the Poisson parameter it becomes a disc-related quantity, and its value may be computed so that flapping responses approximate the N/rev energy of an RBE model. In order to accomplish this the Poisson parameter is determined to be a very small quantity.

Using the Poisson relationships, the flapping angle of a blade may be approximated using the mean values of the cyclic angles. The values required to trim the UH-60 model at various velocities do quite nicely for this purpose. Because the Poisson parameter is very small, the flapping angle of any blade may be approximated in terms of its 1/rev component:

$$\beta = a_0 + \frac{a_2\left(\cos\lambda-\rho\right) - a_1\sin\lambda}{1+\rho^2-2\rho\cos\lambda} \approx a_0 - a_2\rho + \sqrt{a_1^2+a_2^2}\cos\left(\lambda+\phi'\right) \tag{11.1}$$

Here ϕ' is a phase angle. From this expression the 1/rev flapping PSD[14] is shown to be,

Richard McFarland
Comment: These graphs from power.igr. CompPSD.pict

$$P_{1/rev} = \frac{1}{2}\left(a_1^2+a_2^2\right) \approx \frac{1}{2}\left(A_{1F}^2+B_{1F}^2\right) \tag{11.2}$$

[14] Engineering Applications of Correlation and Spectral Analysis, Julius S. Bendat and Allan G. Piersol, John Wiley & Sons, NY, 1980, p. 62.

The PSD at 1/rev was computed from long time histories of the UH-60 model, over a range of velocities. This was accomplished by recording the flapping history of a blade, taking the PSD of the history, and isolating the value for the frequency of 1/rev. This was done for 22 separate velocities, where the mean values of the cyclic angles over the time histories were also recorded. When these two signals are compared the resulting traces are coincident, as shown in Fig. 8.

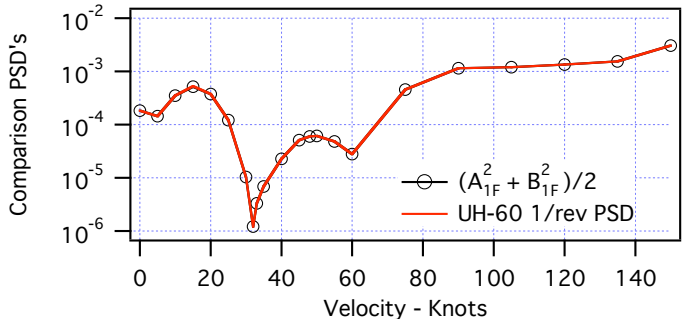

Fig. 8 – Validation of Comparison Technique

This simply validated the technique. Calibrating PSD functions are discussed in Appendix B. The technique may also be used to isolate the N/rev power from the collective time history of A_{0F}. This power may then be compared to values computed using the summed Poisson expression for flapping. The expression is even more accurate in computing N/rev power, because it involves powers of the small Poisson parameter. This signal and the UH-60's power spectral density for the coning angle A_{0F} at 4/rev may then be used to calibrate the Poisson parameter ρ. The approximations used in this process are valid because in the velocity range from hover to 150 knots the value for ρ is never greater than 0.13.

$$\begin{aligned} A_{0F} &= a_0 - a_1 S + a_2 C = a_0 + \frac{\rho^3\left[a_2\left(\cos 4\lambda - \rho^4\right) - a_1 \sin 4\lambda\right]}{1 + \rho^8 - 2\rho^4 \cos 4\lambda} \\ &\approx a_0 - a_2\rho^7 + \rho^3\sqrt{a_1^2 + a_2^2}\cos\left(4\lambda + \phi\right) \end{aligned} \tag{11.3}$$

Here ϕ is a phase angle and for the UH-60 the number of blades N=4. From this expression the PSD of collective at 4/rev is given by,

$$P_{SD}(4/rev) = \frac{1}{2}\left[A_{0F}(4/rev)\right]^2 = \frac{1}{2}\rho^6\left(A_{1F}^2 + B_{1F}^2\right) \tag{11.4}$$

The power spectral density at N/rev is also directly measurable from the UH-60 model. The Poisson parameter for PROMO may therefore be determined from the UH-60 data. The general expression for the Poisson parameter in a rotor system with two or more blades is given by,

$$\rho = \left[\frac{P_{SD}\left(N/rev\right)}{P_{SD}\left(1/rev\right)}\right]^{\frac{1}{2(N-1)}} \tag{11.5}$$

The PSD of A_{0F} was obtained using long time histories, and the value at the 4/rev frequency was determined. This produced $P_{SD}\left(4/rev\right)$. The mean values over the time histories for A_{1F} and B_{1F} were the cyclic angles a_1 and a_2. Hence, the Poisson parameter for the Black Hawk was computed by:

$$\rho = \left[\frac{2P_{SD}\left(4/rev\right)}{A_{1F}^2 + B_{1F}^2}\right]^{\frac{1}{6}} \tag{11.6}$$

The PSD at 4/rev for this model is shown in Fig. 9(a). Also shown by circles in this figure is the PSD computed by PROMO, using the value for the Poisson parameter as computed by Eq. (11.6) and displayed in Fig. 9(b). These are shown as functions of vehicle airspeed.

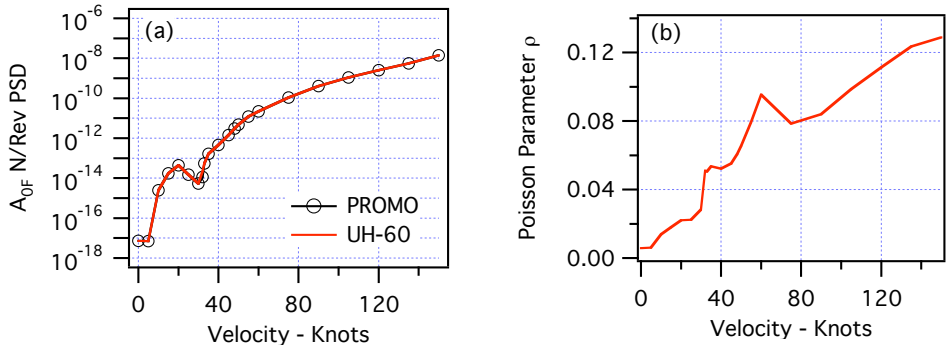

Fig. 9 – PSD and Poisson Parameter

From the above relationships it has been determined that the Poisson parameter for the Black Hawk is the sixth root of the ratio of the 4/rev and 1/rev PSDs. The Poisson parameter then produces excellent power for A_{0F} over the complete velocity range. Using Equations (10.8) and (10.9) the cyclic angles from PROMO may also be computed using the Poisson parameter, and these may be compared with the mean values that are observed for the cyclic angles from the UH-60 model. As shown in Fig. 10(a) and 10(b) they also are in good agreement.

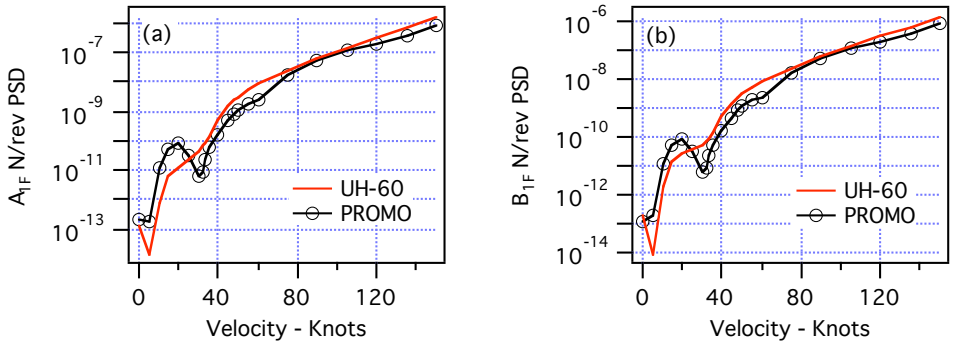

Fig. 10 – N/rev PSDs for the Cyclic Angles

12.0 UH-60 Comparison

The individual flapping angle spectrum decays beyond 4/rev much faster for PROMO than it does for the nonlinear UH-60 model. This is shown in Fig. 11(a), where the thicker curve is from PROMO. The rapid decay has some good consequences. The input collective and cyclic angles assure that the 1/rev power is correct. Since the Poisson parameter

is calibrated at N/rev, the power at this point is also correct. The N/rev power distribution is as shown in Figs. 11(b), (c) and (d). As the blade contributions are summed (and for all axes) the power closely approximates the N/rev magnitudes determined from the Black Hawk simulation.

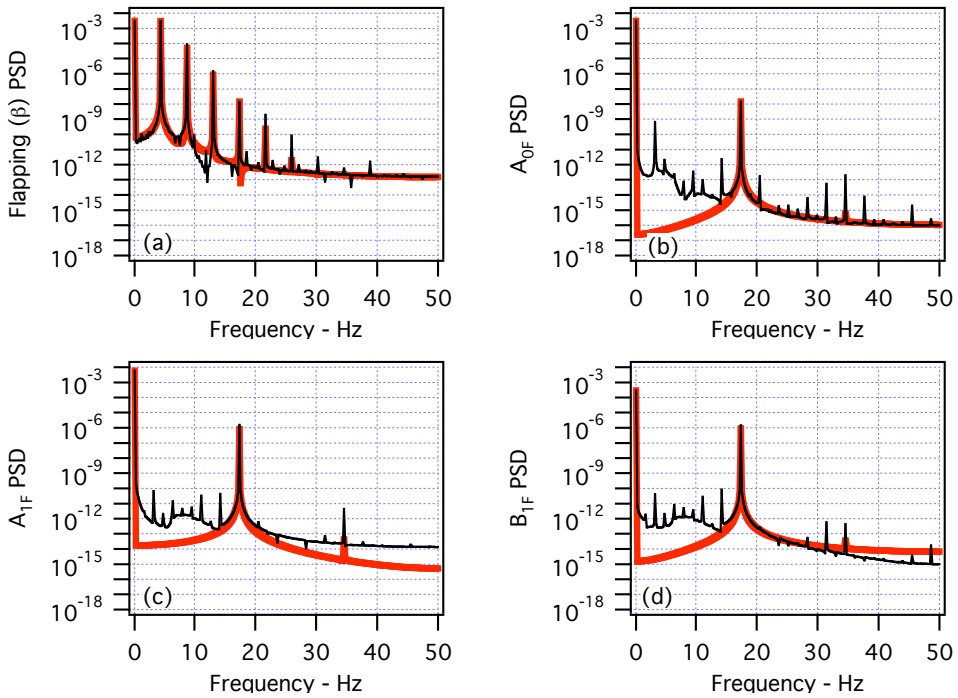

Fig. 11 – Spectral Comparisons at V = 150 Knots

Richard McFarland
Comment: B150.igr created V150Spect.PICT all in data

The UH-60 (thin) curves of Fig. 11 illustrate an adverse feature of discrete, nonlinear models. Due to the aliasing phenomenon, the low-frequency region is contaminated with multiples of N/rev. For example, with a Nyquist Frequency of 50 Hz (at the cycle time of 10 milliseconds) the 6N/rev (103.13 Hz) signal appears at 3.13 Hz, where it appears significantly above the background spectra as shown in Fig. 11(b).

Considering the summed behavior of PROMO, harmonic multiples beyond N/rev quickly vanish. Indeed, the 2N/rev signal is negligible, and may be discarded. From this observation the summed series may be vastly simplified by using the approximations,

$$S = \frac{\rho^{N-1}\sin(N\lambda)}{1-2\rho^{N}\cos(N\lambda)+\rho^{2N}} \approx \rho^{N-1}\sin(N\lambda)$$
$$C = \frac{\rho^{N-1}\left[\cos(N\lambda)-\rho^{N}\right]}{1-2\rho^{N}\cos(N\lambda)+\rho^{2N}} \approx \rho^{N-1}\cos(N\lambda) \qquad (12.1)$$

The series approximations then produce other simplifications,

$$
\begin{aligned}
S_a &= 1+\left(\rho-\frac{1}{\rho}\right)C \approx 1-\rho^{N-2}\left(1-\rho^2\right)\cos(N\lambda) \approx 1-\rho^{N-2}\cos(N\lambda)\\
C_a &= \left(\frac{1}{\rho}-\rho\right)S \approx \rho^{N-2}\left(1-\rho^2\right)\sin(N\lambda) \approx \rho^{N-2}\sin(N\lambda)\\
S_b &= \left(\rho+\frac{1}{\rho}\right)S \approx \rho^{N-2}\left(1+\rho^2\right)\sin(N\lambda) \approx \rho^{N-2}\sin(N\lambda)\\
C_b &= 1+\left(\rho+\frac{1}{\rho}\right)C \approx 1+\rho^{N-2}\left(1+\rho^2\right)\cos(N\lambda) \approx 1+\rho^{N-2}\cos(N\lambda)
\end{aligned}
\qquad (12.2)
$$

Finally, a TPP model may be completely augmented by use of the simple equations:

$$
\begin{aligned}
A_{0F} &\approx a_0+\rho^{N-1}\left[a_2\cos(N\lambda)-a_1\sin(N\lambda)\right]\\
A_{1F} &\approx a_1-\rho^{N-2}\left[a_1\cos(N\lambda)+a_2\sin(N\lambda)\right]\\
B_{1F} &\approx a_2+\rho^{N-2}\left[a_2\cos(N\lambda)-a_1\sin(N\lambda)\right]
\end{aligned}
\qquad (12.3)
$$

Considering the functional form of the Poisson parameter in Fig. 9(b), the value for Poisson's Parameter may be approximated as a straight line from zero at zero velocity, to some value (and beyond) for some other velocity. This is especially true considering the alternative of not producing N/rev signals at all. Hence, the N/rev harmonic power at some non-zero velocity may be sufficient to calibrate the PROMO equations. The larger the velocity that is used, the better the results. Then, because "ρ" is known for all velocities, Equation 12.3 may be used to produce all of the N/rev harmonics of the tip-path plane. The harmonic components of these equations may be separated, and through appropriate scales and transformations may be used to create the vibratory contribution to helicopter motion as isolated to a seat shaker.

CONCLUSIONS

The N/rev harmonics produced by rotor systems and replicated by blade-element models may be approximated in simplified models using relationships derived here. They may be superimposed on disc-plane rotor models, thereby increasing their levels of fidelity and realism. This becomes possible through the use of a single quantity called the "Poisson Parameter," which is a function only of flight speed. The magnitudes and directions of the generated harmonics are appropriate functions of collective and cyclic angles. The mathematical relationships developed here indicate that disc plane models are valid over a wider range of flight conditions than previously assumed.

These techniques produce a capacity that cannot be achieved by simulation using a blade-element model. Rotor system harmonics may be isolated from engineering-level states. Hence, engineering variables as well as a simulator's motion system may be protected from high frequency harmonics. Further, these harmonics are isolated from the integration processes used to create the orientation of the tip-path plane. Because harmonic signals created using Poisson's kernel are computed separately from other dynamics, they are optimal candidates for driving seat shakers.

APPENDIX A – BLADE SUMMATIONS

When rotor variables are expressed as series, double summation is required to create the dynamics of the rotor as a system. The procedure is simple because the order of summation may be shifted. For an arbitrary argument "*x*", the sine and cosine summations over the blade index are given by,

$$\sum_{n=1}^{N}\sin(nx)=\frac{\cos\left[\frac{x}{2}\right]-\cos\left[\left(N+\frac{1}{2}\right)x\right]}{2\sin\left[\frac{x}{2}\right]}$$
$$\sum_{n=1}^{N}\cos(nx)=\frac{\sin\left[\left(N+\frac{1}{2}\right)x\right]-\sin\left[\frac{x}{2}\right]}{2\sin\left[\frac{x}{2}\right]} \tag{A1}$$

From these expressions, the summation of harmonic multiples over the blade index requires the following two series,

$$\sum_{n=1}^{N}\sin\left(\frac{2\pi kn}{N}\right)=\frac{\cos\left(\frac{\pi k}{N}\right)-\cos(2\pi k)\cos\left(\frac{\pi k}{N}\right)+\sin(2\pi k)\sin\left(\frac{\pi k}{N}\right)}{2\sin\left(\frac{\pi k}{N}\right)}=0 \tag{A2}$$

$$\sum_{n=1}^{N}\cos\left(\frac{2\pi kn}{N}\right)=\frac{\sin(2\pi k)\cos\left(\frac{\pi k}{N}\right)+\cos(2\pi k)\sin\left(\frac{\pi k}{N}\right)-\sin\left(\frac{\pi k}{N}\right)}{2\sin\left(\frac{\pi k}{N}\right)}=\begin{cases}N & \frac{k}{N}=m\\ 0 & \frac{k}{N}\neq m\end{cases} \tag{A3}$$

The summed sine series always vanishes. Providing that $k/N\neq m$ (where *m* is any integer), the cosine sum also vanishes. When the k/N ratio is an integer, however, the cosine series is equal to *N*. Hence the summed trigonometric series of an advance angle do not vanish for frequencies that are multiples of the number of blades. The trigonometric summations of multiples of the advance angle are given by,

$$\sum_{n=1}^{N}\sin\left(k\lambda_n\right)=\sum_{n=1}^{N}\sin\left[k\left(\lambda+\frac{2\pi n}{N}\right)\right]=\begin{cases}N\sin(mN\lambda) & \frac{k}{N}=m\\ 0 & \text{otherwise}\end{cases} \tag{A4}$$

$$\sum_{n=1}^{N}\cos\left(k\lambda_n\right)=\sum_{n=1}^{N}\cos\left[k\left(\lambda+\frac{2\pi n}{N}\right)\right]=\begin{cases}N\cos(mN\lambda) & \frac{k}{N}=m\\ 0 & \text{otherwise}\end{cases} \tag{A5}$$

The summations illustrate that for simple trigonometric relationships all harmonic terms vanish when summed over the blade index, except for RPM multiples of the number of blades.

APPENDIX B – PSD OPERATIONS

Classical turbulence filters are functions of the vehicle airspeed V and the characteristic wavelength L of the turbulence. These parameters define a parameter $c = L/V$. Turbulence filters may be used to calibrate Power Spectral Density operations. This is possible because they are normalized so the integral over all frequencies of the PSD equals unity. When the standard deviation is explicitly included in the filter, the integral (or area) of the PSD then becomes the variance σ^2. Turbulence filters usually originate from their spectral density functions. A vertical turbulence filter $f(s)$ that includes the standard deviation σ, for example, is represented by its spectral density function,

$$\left|f(j\omega)\right|^2 = \frac{\sigma^2 L\left[1+3\left(\frac{L\omega}{V}\right)^2\right]}{V\pi\left[1+\left(\frac{L\omega}{V}\right)^2\right]^2} = \frac{\sigma^2 c\left[1+3c^2\omega^2\right]}{\pi\left[1+c^2\omega^2\right]^2} = \frac{\sigma^2 c\left(1+j\sqrt{3}c\omega\right)\left(1-j\sqrt{3}c\omega\right)}{\pi\left[(1+jc\omega)(1-jc\omega)\right]^2} \tag{B1}$$

The integral of this function over all frequencies then produces the variance:

$$\int_0^\infty \left|f(j\omega)\right|^2 d\omega = \frac{\sigma^2 c}{\pi}\int_0^\infty \frac{1+3c^2\omega^2}{\left(1+c^2\omega^2\right)^2}d\omega = \frac{\sigma^2}{\pi}\int_0^\infty \frac{1+3x^2}{\left(1+x^2\right)^2}dx = \frac{\sigma^2}{\pi}\int_0^\infty \frac{dx}{\left(1+x^2\right)^2} + \frac{3\sigma^2}{\pi}\int_0^\infty \frac{x^2 dx}{\left(1+x^2\right)^2}$$

$$= \frac{\sigma^2}{\pi}\int_0^\infty \frac{dx}{\left(1+x^2\right)^2} + \frac{3\sigma^2}{2\pi}\int_0^\infty \frac{dx}{1+x^2} = \frac{\sigma^2}{2\pi}\int_0^\infty \frac{dx}{1+x^2} + \frac{3\sigma^2}{2\pi}\int_0^\infty \frac{dx}{1+x^2} = \frac{2\sigma^2}{\pi}\int_0^\infty \frac{dx}{1+x^2} \tag{B2}$$

$$= \frac{2\sigma^2}{\pi}\tan^{-1}(x)\Big|_0^\infty = \sigma^2$$

For discrete operations, the integral of the spectral density function may be approximated by the summation,

$$\int_0^\infty \left|f(j\omega)\right|^2 d\omega \approx \frac{\sigma^2 c}{\pi}\sum_1^N \frac{\left[1+3c^2\omega^2\right]}{\left[1+c^2\omega^2\right]^2}\Delta\omega \tag{B3}$$

This should closely approximate σ^2 if a sufficient number of frequency evaluations N are performed.

The transfer function itself is obtained from a decomposition of the spectral density function of Equation (B1):

$$f(s) = \sigma\sqrt{\frac{c}{\pi}}\frac{\left(\sqrt{3}cs+1\right)}{(1+cs)^2} \tag{B4}$$

In simulation, the function is driven by a Gaussian noise source with unity variance, so that the integrated output spectrum has the desired variance σ^2. The time history of turbulence is then analyzed by FFT software. Consider the LabVIEW PSD program called "Auto Power Spectrum" from National Instruments[15] that initially produces the two-sided autospectral density function,

$$S_{xx}(f) = E\left[\left|X(f)\right|^2\right] = \frac{FFT^*(Signal)\times FFT(Signal)}{N^2} \tag{B5}$$

where N is the number of samples in the input sequence. This program (or "VI", for "Virtual Instrument") then converts this into a single-sided power spectrum.

---

[15] National Instruments Corp., Austin, TX, infor@ni.com, www.ni.com, Version 6.0, July 2000.

$$G_{xx}(k\Delta f) = \begin{cases} 0 & k < 0 \\ S_{xx}(0) & k = 0 \\ 2S_{xx}(k\Delta f) & 0 < k \le N/2 \end{cases} \tag{B6}$$

The sample frequency is given by the inverse of the cycle time $f_{Sample} = 1/h$. The frequency increment in the units of Hertz or radians per second are given by,

$$\Delta f = \frac{f_{Sample}}{N} \qquad \Delta\omega = 2\pi\,\Delta f \tag{B7}$$

The number of frequency points that are produced by this operation is one-half the number of time-series data points. Hence, the maximum frequency abscissa for the PSD is one-half of the sample frequency, also known as the Nyquist frequency. The outputs of the software are in the units of the input signal squared. In the conversion from two-sided to single-sided spectra,[16] *N* time points produce *N/2* frequency domain points which are summed and scaled times the entire Nyquist range. This produces an estimate of the variance.

$$\sigma^2 = \frac{N}{2}\sum_{n=1}^{N/2} G_{xx}(n\Delta f)\Delta\omega \tag{B8}$$

The finite Fourier transforms of the original time history records are actually subdivided into a number of sequential records in order to create more concise estimates of the spectral density functions.[17]

---

[16] Nonlinear System Analysis & Identification from Random Data, Julius S. Bendat, John Wiley & Sons, NY, 1990, p. 11.

[17] Engineering Applications of Correlation and Spectral Analysis, Julius S. Bendat and Allan G. Peirsol, John Wiley & Sons, NY, 1980, p. 72.